Technical Note

Contact Force- and Amplitude-Controllable Vibrating Probe for Somatosensory Mapping of Plantar Afferences With fMRI

Eugen Gallasch, PhD,[1]* Stefan M. Golaszewski, MD,[2,4] Martin Fend,[1] Christian M. Siedentopf,[3,4] Florian Koppelstaetter, MD,[3,4] Wilhelm Eisner, MD,[5] Franz Gerstenbrand, MD,[6] and Stephan R. Felber, MD[3]

Purpose: To study cerebral responses evoked from mechanoreceptors in the human foot sole using a computer-controlled vibrotactile stimulation system.

Materials and Methods: The stimulation system consisted of two stationary moving magnet actuators with indentors to gently contact and vibrate the foot sole during functional MRI (fMRI) experiments. To allow independent settings of contact force (0–20 N) and intensity of vibration (frequency range = 20–100 Hz) the actuators were controlled by a digital servo loop. For fMRI experiments with complex stimulus protocols, both vibrating probes were further operated under supervisory control.

Results: The MR compatibility of this electromagnetic system was tested in a 1.5T scanner with an actively shielded magnet (Siemens Magnetom Sonata). Blood oxygenation level-dependent (BOLD) responses were detected in the contralateral left pre- and postcentral gyrus, bilaterally within the secondary somatosensory cortex, bilaterally within the supplementary motor cortex, and bilaterally within the anterior cingular gyrus.

Conclusion: This stimulation device provides a new tool for identifying cerebral structures that convey sensory information from the foot region, which is of promising diagnostic value, particularly for assessing sensorimotor deficits resulting from brain lesions.

Key Words: fMRI; vibrotactile stimulation; sensorimotor cortex; neurodiagnostics; active vibration control; MR compatibility

J. Magn. Reson. Imaging 2006;24:1177–1182.

THE HUMAN BRAIN receives multiple types of afferent information from body surfaces, and a large proportion of this information originates from cutaneous mechanoreceptors. Vibrotactile stimulation of these receptors results in specific cortical activations that are associated with a short-latency hemodynamic response (1), and provides a rationale for reproducible somatosensory mapping (2,3). Somatosensory mapping with functional MRI (fMRI) has clinical potential to testing the intactness of nerve conduction and characterizing neuronal function adjacent to brain lesions.

Somatosensory mapping requires the use of MR-compatible devices to deliver well controlled and reproducible vibration stimuli. Various devices have been proposed for the arm, hand, and fingers, such as pneumatically-driven air bags (4,5), piezodisks (6,7), cable-driven rotating masses (8), and even coil designs utilizing the scanner-internal static magnetic field (9). However, these devices are less suitable for the human foot sole. One reason for this is that sole afferences have a lower sensitivity (10) and therefore more powerful stimuli are needed to elicit sensorimotor responses. Another reason is that under normal conditions (e.g., standing and walking) the foot sole is under steady or time-varying gravitational load. Thus, the functional stimulation of foot-sole receptors calls for a device that is capable of delivering gait-like and bipedal stimulation patterns while the subject is lying in the scanner. In a first approach to such demands, we focused developing on a stationary device that delivers programmed con-

[1]Department of Physiology, Medical University Graz, Graz, Austria.
[2]Department of Neurology, Paracelsus Medical University Salzburg, Salzburg, Austria.
[3]Department of Neuroradiology, Medical University Innsbruck, Innsbruck, Austria.
[4]fMRI Laboratory, Department of Psychiatry, Medical University Innsbruck, Innsbruck, Austria.
[5]Department of Neurosurgery, Medical University Innsbruck, Innsbruck, Austria.
[6]Ludwig Boltzmann Institute for Restorative Neurology and Neuromodulation, Vienna, Austria.

Contract grant sponsor: Austrian National Bank; Contract grant number: 10109; Contract grant sponsor: Austrian Ministry for Education, Science and Culture; Contract grant number: 140.607.

*Address reprint requests to: E.G., Department of Physiology, Medical University of Graz, Harrachgasse 21/5, 8010 Graz, Austria. E-mail: eugen.gallasch@meduni-graz.at

Received May 29, 2005; Accepted July 28, 2006.

DOI 10.1002/jmri.20742
Published online 9 October 2006 in Wiley InterScience (www.interscience.wiley.com).

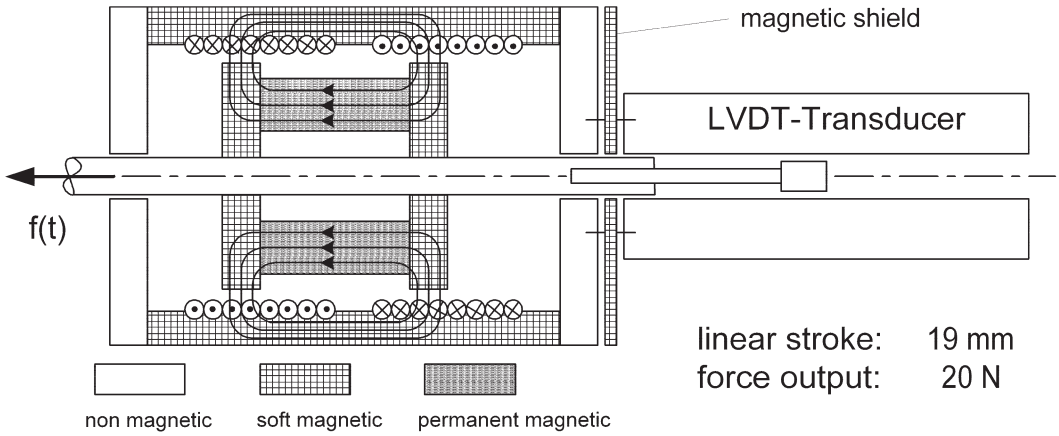

Figure 1. Mechanics of the moving magnet actuator with attached displacement transducer for vibration control (cross-sectional plot).

tact forces during amplitude-controlled vibratile stimuli.

Because of the relatively long distance between the sole and the cortex, electrodynamic devices have been taken into consideration. These actuator types are linear in their input-output characteristic, which makes them suitable for producing well-controlled and powerful stimulation patterns. In this paper we describe a stationary moving magnet actuator with an indentor to contact and vibrate the sole of the foot. Special attention was paid to the control of the actuator to allow independent settings of contact force and vibration. Further, a two-actuator system was set up for fMRI paradigms with more complex stimulation patterns. Attention was also paid to the safety aspects of this system working within the MR environment.

MATERIALS AND METHODS

Actuator and Control Design

For vibrotactile stimulation by indentation, the human foot sole is considered to represent a soft elastic material with a certain tissue thickness and stiffness. Plantar tissue thickness was determined in healthy subjects ranging from 8 mm (big toe) to 16 mm (heel), and stiffness was characterized by Young's moduli from 50 (heel) to 150 (first metatarsol head (MTH) at an indentation depth within 10% of the initial thickness (11). For a flat- ended cylindrical indentor of 1 cm^2, the indentation force is then about 5 N (heel), corresponding to a local stiffness of about 3.1 N/mm. Considering factors such as the creep of loaded tissue and compliance of toe joints, an actuator with an output force of 20 N at a stroke of 20 mm should be well suited for this application.

A commercially available linear moving-magnet device with a stroke of 19 mm and a force output of 20 N (type LMNM2-1F5-F8; Baldor Inc., USA) was selected as the actuator. This actuator consists of an axially magnetized permanent magnet suspended in a soft magnetic tube with two antiparallel-winded stator coils (Fig. 1). By means of this concentric design, radial and axial attracting forces on the magnet disappear and the actuator becomes highly "back-drivable" (i.e., no forces are produced when the magnet is driven by external forces). For vibration control, one end of the actuator shaft is connected to an LVDT position sensor (type 1002 XS-D; Lucas-Scheavitz, UK) and the second free end is connected to the indentor. The actuated mass without the indentor is 0.18 kg. The total mass of each sensor-actuator is 1.1 kg with a length of 20 cm and a diameter of 5 cm.

The output force $f(t)$ produced by the current $i(t)$ in the stator coil, and the resulting magnetic field B in the air gap is given by the Lorentz force law:

$$f(t) = i(t) \times B \quad (1)$$

To avoid motion-induced friction from the back electromotive force (EMF), the stator coil is powered by a current amplifier. This feature preserves back-drivability and proved advantageous in keeping the indentor in contact with the sole during small foot motions while the subject was lying in the scanner.

To allow independent settings of contact force $f_{in}(t)$ and vibration $x_{in}(t)$, we designed a servo controller (see Fig. 2). It consists of a velocity feedback loop and includes a summing stage in the forward control path to set the contact force. Further input to the forward path comes from the reaction forces of the indented tissue. The velocity of the moving magnet is obtained from differentiation of the transducer signal $x(t)$, and since the desired vibration intensity is given by displacement, this input signal also has be differentiated. Because the contact force has a static nature (0–1 Hz), this second input signal does not conflict with vibration control.

A critical parameter in this control design is the loop gain k, which has the dimension of a mechanical impedance (frequency response function of force/velocity). This gain should be high enough to impede reactive forces from the vibrated sole in a frequency range of 20–100 Hz. The dynamic stiffness (frequency response function of force/displacement) of the controlled system is contained in the force to displacement transfer function:

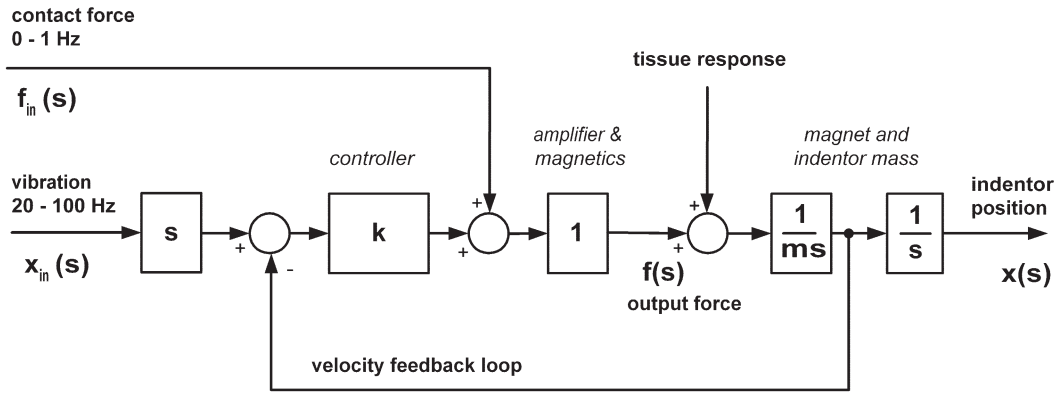

Figure 2. Control block scheme (Laplace transformed operations) for independent settings of contact force and vibration.

$$L\left\{\frac{f(t)}{x(t)}\right\} = T(s) = s(sm + k) \tag{2}$$

By inserting the angular frequency $j\omega$ into the Laplace operator s, we then obtain the absolute valued frequency response by

$$|T(j\omega)| = \sqrt{\omega^4 m^2 + \omega^2 k^2} \tag{3}$$

To determine the loop gain, a dynamic stiffness five times higher than the expected stiffness of the sole was assumed (3 N/mm, see above). Since the dynamic stiffness given by Eq. [3] increases with frequency, the loop gain was determined at 20 Hz. With $m = 0.20$ kg (mass of moving magnet and indentor) and $T_{20Hz} = 15$ N/mm, a loop gain of $k = 117$ was found. This control design was implemented by software running on a standard PC (SUSE Linux operating system with an RT kernel and 5-kHz process cycle). Therefore, the control signals were digitized by 16 bit AD/ DA converters and interfaced to the PC parallel port.

To test the performance of the implemented controller, a piece of foam rubber with material properties similar to those of sole tissue (initial stiffness = ~3 N/mm) was indented and vibrated (see Fig. 3, left). The vibration frequency was stepwise increased from 10 to 250 Hz at a given amplitude of 0.4 mm. To study the influence of contact force on vibration amplitude, three load levels (2, 5, and 10 N) were tested.

In Fig. 3 (right) the open and closed loop frequency responses are shown. Without velocity feedback (open loop), the vibration amplitude depends highly on the frequency and contact force. With velocity feedback ($k = 120$), the force dependence becomes small, and an almost flat frequency response between 20 and 100 Hz is obtained.

Setup for Scanning and Operation Modes

The complete stimulation hardware consists of the platform with foot supports, the two vibration probes, cables, and the remote in/out unit with the PC (see Fig. 4). For safety reasons and to avoid mechanical resonance, the platform consists of a rigid aluminum plate (thickness = 10 mm, length = 98 cm, width = 49 cm). The lower side of the platform is equipped with rubber elements that fit tightly into the sled of the scanner. Two supports (one for the ankle and one for the foot) are used to keep the leg in a relaxed, stable position. Both

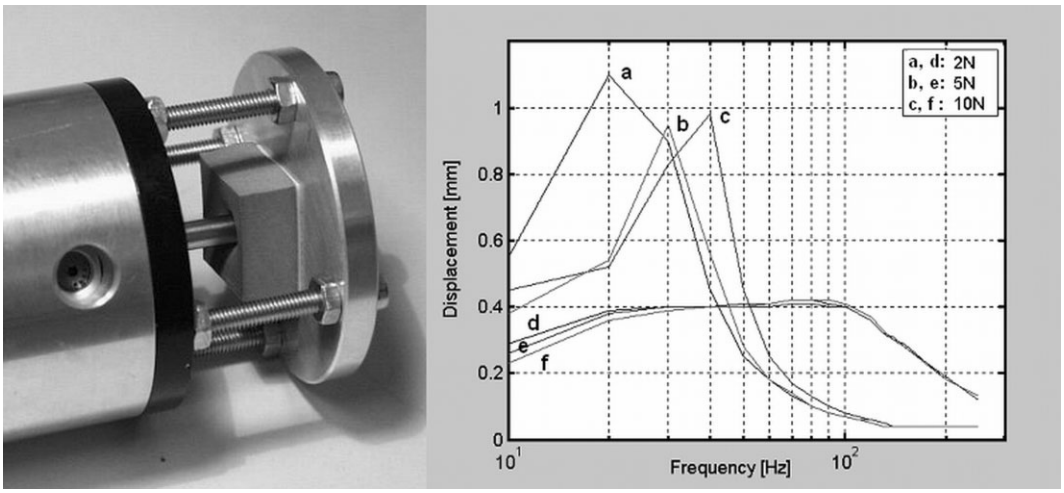

Figure 3. Test of vibration control with a soft elastic specimen as the test object. The diagram shows the open-loop (**a–c**) and closed-loop (**d–f**) frequency responses with indentation force as a parameter.

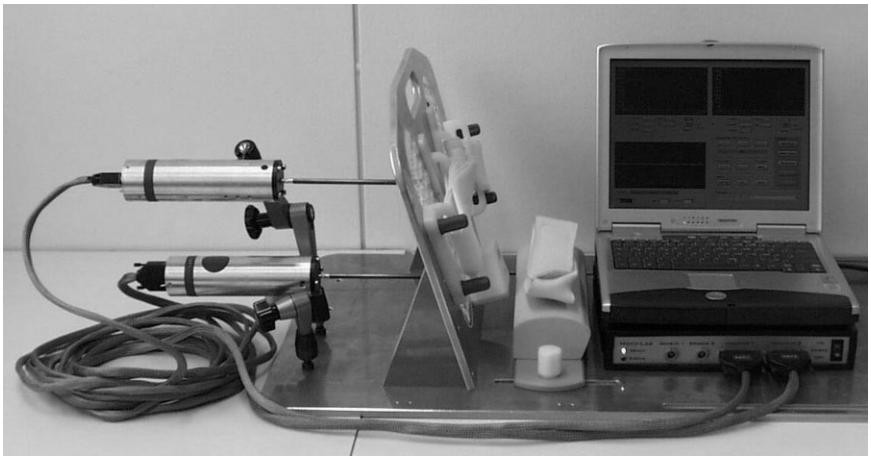

Figure 4. Hardware of the stimulation system consisting of a platform with vibrating probes connected via long cables to the in/out unit and computer.

supports are equipped with Velcro bands for quick fixation. Exchangeable foot-shaped, plexiglass sections with 30-mm holes are used to contact and vibrate the sole by the indentors.

To avoid accidental risk caused by magnetic translation, both vibration probes are fix-mounted on the platform via nonmagnetic adjustable stands (type SG, Tekusa Inc., Switzerland). These stands consist of two permanently connected joint levers with a hand-wheel actuated release mechanism for positional adjustment of the probes. After this mechanism is gripped, the joints become locked, thus providing excellent mechanical grounding of the probes. To prevent magnetic translation of the whole stimulation system, two additional brackets with screws are used to clamp the platform to the sled.

To minimize RF emissions during operation of the stimulation system, the in/out unit and the PC are installed outside the scanner room. The in/out unit includes an AD/DA-interface board with analog filters (1.0 kHz, Butterworth fourth order) and voltage-controlled current amplifiers to drive the moving magnet devices. Analog amplifiers (type LSC 30/2; Maxon Inc., Switzerland) were used to avoid the spike noise that is typically produced by switched power devices. Shielded multi-cables (10 m) were used to connect the vibrating probes to the in/out unit.

In addition to process control, the PC software includes features for stimulus synthesis and sequencing, as well as master-slave and communication capabilities. For one- and two-level stimulation protocols (on/off and difference effects), the stimulator is operated asynchronously to MR sequencing (block design). For stimulus-response protocols with multiple levels, which also may include vision and audition, event-related stimulation designs (12) are advantageous. In the present study we used commercially available software (Presentation, V0.5; Neurobehavioral Systems, USA) for synchronization, stimulus sequencing, and stimulus allocation.

To work with event-related designs, the stimulator is operated in the slave mode. For master-slave operation, a software communication protocol with codes for stimulus frequency, amplitude, and contact force was defined. For data exchange between master and slave PC, currently the serial port (RS 232) is used. The PC software also includes scope and alarm functions to survey the indentor's motions during stimulus delivery, as well as backup and quick-look capabilities for documentation.

RESULTS

MR Compatibility

Since ferromagnetic materials are contained in the stimulation devices[1], special emphasis was put on MR compatibility and safety. According to the safety guidelines issued by GE Medical Systems (13) and others (14,15), a device is labeled MR safe if it can be demonstrated that when the device is introduced or used in the MR scan room, it does not pose an increased safety risk to the patient and staff. Before a device can be labeled MR-compatible, it must be further demonstrated that it performs its intended function without performance degradation. For MR compatibility, further effects on devices and imaging have to be differentiated. Among the effects on devices are induced static magnetization, torque, and translational forces. According to the guidelines mentioned above, ferromagnetic materials should be operated in zone 4, behind the 20-mT line. In this zone the effects on devices become small.

To determine the minimal distance for safe operation of the vibrating probes, we used a Gaussmeter (model 5080; Bell Inc., USA) to measure the magnetic field along the z-axis from two 1.5T MRTs with actively shielded magnets (Siemens Magnetom Sonata and Phillips Gyroscan). In the case of the Phillips Gyroscan, the 20-mT line was at 1.9 m, and in the case of the Siemens Sonata, this line was at 2.1 m from the center of the magnet. These results were also reflected in practical experience. Because of the induced magnetization, it was difficult to operate the vibration probes in front of smaller subjects (body length < 1.80 m) in the Sonata. This problem could be resolved with the use of longer indentors (20 cm).

[1]The total ferromagnetic mass contained in each device is 570 grams.

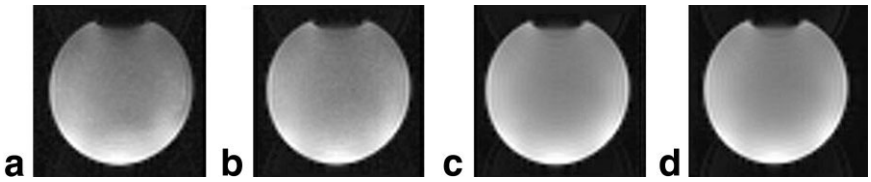

Figure 5. Effects on imaging tested by EPI scans acquired from a spherical NaCl phantom: (**a**) stimulator in the MR room with power on, (**b**) stimulator operated with an amplitude of 1 mm and a frequency of 50 Hz, (**c**) operation with shielding and grounding of the cables, and (**d**) stimulator not present in the MR room.

To estimate effects on imaging, EPI scans with the same acquisition parameters as described below were acquired from a spherical NaCl phantom (see Fig. 5). During the first scan the stimulator was present within the MR room with the power on, but was not operated (Fig. 5a). During the second scan the stimulator was operated with an amplitude of 1 mm and a frequency of 50 Hz (Fig. 5b). RF emissions produced by a DC/DC converter and radiated via the cable were identified as the source of elevated noise. Additional shielding and grounding of the cables reduced the RF emissions (Fig. 5c), resulting in an imaging quality similar to that obtained with the stimulator outside of the MR room (Fig. 5d).

Imaging Tests

To test the diagnostic functionality of the stimulation system, imaging experiments were performed with the 1.5 T Magnetom Sonata equipped with an EPI-capable gradient system (rise time = 300 μsec, gradient strength = 25 mT/msec) and a circularly polarized head coil (FOV = 250 mm). Five healthy male volunteers with right-foot dominance and no history of neurological, psychiatric, or internal disorders were tested. The study was approved by the local ethics committee. The subjects were instructed to remain relaxed, place their hands above their abdomen, and keep their eyes closed during the fMRI recordings. Foam padding and a special helmet fixed to the head coil were used to limit involuntary head motions for the duration of the recordings.

A complete experimental run consisted of two parts. In the first part, the subjects performed self-paced movements of about 2 Hz with the right foot. This movement sequence was utilized to emphasize a BOLD contrast associated with neuronal activation in order to test the functionality of the fMRI system (the on/off motor paradigm). In the second part, 50 Hz vibrations with an amplitude of 1 mm and a contact force of 5 N were applied to the sole of the right foot above the basic joint of digit I (the vibration paradigm). The contact area between the skin surface and the indentor was circular and exactly 0.5 cm^2.

For fMRI we employed T2*-weighted single-shot echo-planar sequences (TR/TE/α = 0.96 msec/66 msec/90°, matrix = 128 × 128, voxel dimension = 1.95 × 1.95 × 3.8 mm) (16). We acquired 30 slices parallel to the bicommissural plane. Series of five stacks of images during vibration (condition A) were alternated with five stacks of images at rest (condition B) up to a total volume of 45 stacks of images (time series: BABAB-ABAB). The scan TR for the task/rest conditions was six seconds.

The vibration paradigm led to the cortical activation pattern shown in Fig. 6. Within-group analysis of the vibration data of the five subjects on the first level shows a blood oxygenation level-dependent (BOLD) response: 1) contralaterally to the vibrated foot within the primary sensorimotor cortex SM1 (pre- and postcentral gyrus, Brodmann area (BA) 3a, b, 2, 1, and 4); 2) bilaterally within the secondary somatosensory cortex S2 within the inferior parietal and superior temporal region (inferior parietal lobule, superior temporal gyrus, BA 39, 40, 21, and 22); 3) bilaterally within the superior frontal gyrus within the supplementary motor area SMA (superior frontal gyrus, medial BA 6); and 4) bilaterally within the anterior cingulate gyrus GC (BA 32).

DISCUSSION

In this paper we have described a stationary vibrotactile stimulator for somatosensory mapping. A key feature of

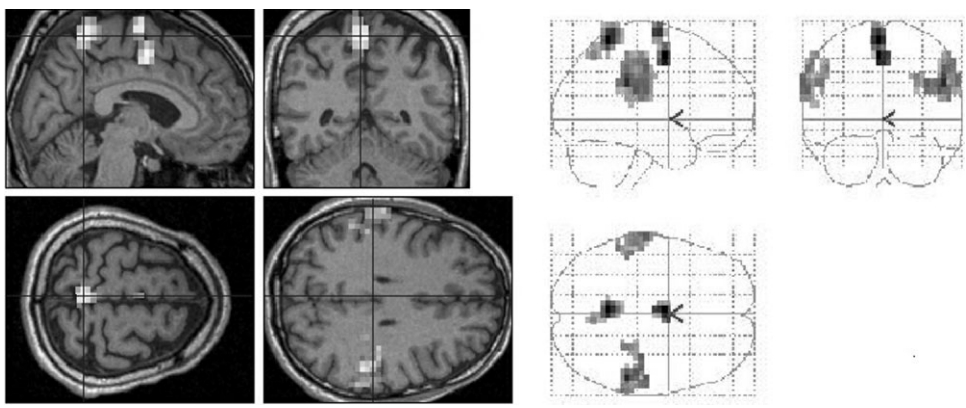

Figure 6. fMRI map (group data for five subjects) for vibrotactile stimulation of the foot sole with a vibration frequency of 50 Hz and a vibration amplitude of 1 mm with a sinusoidal stimulus waveform. A fixed-effects analysis was performed on a cluster level for $k > 20$ and $P < 0.05$, corrected for multiple comparisons.

this stimulator is that contact force and vibration can be programmed independently, which reduces systematic errors in stimulation tests. Previous nonstationary devices (4–9) required an active motor component to contact the vibrating probe, and this was shown to be a source of systematic errors (17). Such errors can be reduced by amplitude control. As shown by the specimen test, the vibration amplitude is conserved against responding tissue forces. By measuring the indentation depth at a given force, one can quantify plantar stiffness at the stimulation site. This may be important for establishing more quantitative stimulus-response relationships as a reference for diagnostic procedures.

From the results regarding MR compatibility, we conclude that linear electromagnetic devices can be operated behind the 20-mT line with minimal effects on imaging and performance. We kept the effects on imaging small by utilizing analog electronics and limiting the control bandwidth (0–1 kHz). With respect to safety, it should be noted that the field gradient of a typical 1.5T scanner quickly increases inside the 20-mT line, causing a strong magnetic pull. The preservation of safety, therefore, requires constant vigilance to ensure that the platform with devices is not inadvertently moved too close to the center of magnet. Only informed research personnel together with an MR health-care professional should work with this stimulator.

The preliminary results of the fMRI imaging experiments show that this electromagnetic device is well suited for eliciting vibration-induced changes of cerebral blood flow within a standard MR environment. The observed brain activation within the network of the sensorimotor cortex indicates that the device may be useful for neurophysiological research (e.g., experiments on weightlessness), as well as functional diagnoses of the brain in a clinical context. Possible applications include preoperative micromapping of the sensorimotor cortex in patients with brain tumors, investigating brain plasticity and reorganization in neurorehabilitation (18), studying patients in comatose and vegetative states (19,20), and assessing the afferent pathways after spinal cord injury.

The ability to operate the probes from a stationary platform provides several experimental opportunities. One is simultaneous operation of multiple probes—for example, to investigate two-point discrimination, or to simulate functional tactile patterns as produced during standing or walking. Furthermore, the tips of the indentors can be equipped with secondary devices, such as electrodes, to deliver electrical stimuli, or with Peltier elements to evoke responses in warm-cold receptors. Such multimodal test designs also have a diagnostic potential for various disorders, such as sensory deficits in the lower extremities (e.g., diabetic neuropathies, in which early sensory deficits appear on the foot sole).

In conclusion, the proposed force- and amplitude-controllable stimulation system opens new possibilities for identifying cerebral structures that convey sensory information from the foot region. Together with other neurophysiological techniques, this approach could contribute to a better understanding of how this information becomes altered by different pathologies.

REFERENCES

1. Logothetis NK, Pauls J, Augath M, Trinath T, Oeltermann A. Neurophysiological investigation of the basis of the fMRI signal. Nature 2004;412:150–157.
2. Sakai K, Watanabe E, Onodera Y, et al. Functional mapping of the human somatosensory cortex with echo-planar MRI. Magn Reson Med 1995;33:736–743.
3. Servos P, Zacks J, Rummelhart DE, Glover GH. Somatotopy of the human arm using fMRI. Neuroreport 1998;9:605–609.
4. Stippich Ch, Hofmann R, Kapfer, et al. Somatotopic mapping of the human primary somatosensory cortex by fully automated tactile stimulation using functional magnetic resonance imaging. Neurosci Lett 1999;277:25–28.
5. Golaszewski SM, Zschiegner F, Siedentopf CM, et al. A new pneumatic vibrator for functional MRI of the human sensorimotor cortex. Neurosci Lett 2002;324:125–128.
6. Maldjian JA, Gottschalk A, Patel RS, Pincus D, Detre JA, Alsop CD. Mapping of secondary somatosensory cortex activation induced by vibrational stimulation—an fMRI study. Brain Res 1999;824:291–295.
7. Harrington GS, Calvin TW, Diwns JH. A new vibrotactile stimulator for functional MRI. Hum Brain Mapp 2000;10:140–145.
8. Golaszewski SM, Siedentopf CM, Baldauf E, et al. Functional magnetic resonance imaging of the human sensorimotor cortex using a novel vibrotactile stimulator. Neuroimage 2002;17:421–430.
9. Graham SJ, Staines WR, Nelson A, Plewes DB, Mcllry WE. New devices to deliver somatosensory stimuli during functional MRI. Magn Res Med 2001;46:436–442.
10. Kennedy PM, Inglis JT. Distribution and behavior of glabrous cutaneous receptors in the human foot sole. J Physiol 2002;538:995–1002.
11. Zheng YP, Choi YKC, Wong K, Chang S, Mak AFT. Biomechanical assessment of plantar foot tissue in diabetic patients using an ultrasound indentation system. Ultrasound Med Biol 2000;26:451–456.
12. Dale A, Buckner R. Selective averaging of rapidly presented individual trails using fMRI. Hum Brain Mapp 2002;5:329–340.
13. GE Medical Systems. MR safety and MR compatibility. http://www.ge.com/medical/mr/iomri/safety.htm; 1997.
14. Chinzei K, Kikinis R, Jolesz F. MR compatibility of mechatronic devices, design criteria. Proceedings of the MICCA 99. Lecture Notes Comput Sci 1999;1679:1020–1031.
15. Shellock FG. Magnetic resonance safety update 2002, implants and devices. J Magn Reson Imaging 2002;16:485–496.
16. Kwong KK. Functional magnetic resonance imaging with echo planar imaging. Magn Reson Q 1995;11:1–20.
17. Wu JZ, Dong RG, Schopper AW, Smutz WP. Analysis of skin deformation profiles during sinusoidal vibration of fingerpad. Ann Biomed Eng 2003;31:867–878.
18. Pons TP, Garraghty PE, Mishkin M. Serial and parallel processing of tactual information in somatosensory cortex of rhesus monkeys. J Neurophysiol 1992;68:518–527.
19. Kampfl A, Schmutzhard E, Franz G, et al. Prediction of recovery from post-traumatic vegetative state with cerebral magnetic resonance imaging. Lancet 1998;35:1763–1767.
20. Laureys S, Faymonville ME, Peigneux P, et al. Cortical processing of noxious somatosensory stimuli in the persistent vegetative state. Neuroimage 2002;17:732–741.